Zheng Jie (Orcid ID: 0000-0002-4161-627X)

cao zhengyu (Orcid ID: 0000-0002-2692-2949)

Surfactant cocamide monoethanolamide causes eye irritation by activating nociceptor TRPV1

Running title: Mechanism of cocamide monoethanolamide-induced eye irritation

Fang Zhao[1,‡], Shuangyan Wang[1,‡], Yan Li[1], Jin Wang[2], Yujing Wang[1], Chunlei Zhang[1], Yong Li[3], Longjiang Huang[4], Ye Yu[2,*], Jie Zheng[5], Boyang Yu[1], Isaac N Pessah[6,*], and Zhengyu Cao[1,*]

[1]*State Key Laboratory of Natural Medicines and Department of TCM pharmacology, School of Traditional Pharmacy, China Pharmaceutical University, Nanjing, Jiangsu, China, 211198*

[2]*Department of Basic Medicine, School of Basic Medicine and Clinic Pharmacy, China Pharmaceutical University, Nanjing, Jiangsu, China, 211198*

[3]*Department of Biochemistry and Molecular Cell Biology, Shanghai Key Laboratory for Tumor Microenvironment and Inflammation, Institute of Medical Sciences, Shanghai Jiao Tong University School of Medicine, Shanghai, China, 200025*

[4]*College of Chemical Engineering, Qingdao University of Science and Technology, Qingdao, China, 266042*

[5]*Department of Physiology and Membrane Biology, University of California, Davis, CA, USA, 95616*

[6]*Department of Molecular Bioscience, School of Veterinary Medicine, University of California, Davis, California, USA, 95616*

[‡], equal contribution

**** Correspondence:***

Zhengyu Cao, Ph.D.

Department of TCM Pharmacology, School of Traditional Chinese Pharmacy, China Pharmaceutical University, Nanjing, Jiangsu, China, 211198

E-mail: zycao@cpu.edu.cn

Isaac N Pessah

Department of Molecular Bioscience, School of Veterinary Medicine, University of California, Davis, California, USA, 95616

This article has been accepted for publication and undergone full peer review but has not been through the copyediting, typesetting, pagination and proofreading process which may lead to differences between this version and the Version of Record. Please cite this article as doi: 10.1111/bph.15491

E-mail: inpessah@ucdavis.edu

***Ye Yu,* Ph.D.**

Department of Basic Medicine, School of Basic Medicine and Clinic Pharmacy, China Pharmaceutical University, Nanjing, Jiangsu, China, 211198

E-mail: yuye@shsmu.edu.cn

Word count: *6641*

Acknowledgments

Funding: This work was supported by National Key R&D program of China (No. 2018YFF0215200); National Natural Science Foundation of China (No. 81903826, 81972960); the Innovative Drug Development Program from Department of Science and Technology (2018ZX09101003-004-002); China Postdoctoral Science Foundation (2018M642371); "Double First-Class" University project (CPU2018GF06), joint project between China Pharmaceutical University and East South University (2242019K3DZ01); and National Institutes of Environmental Health Sciences (P42 ES004699 and 1R01 ES030318) and the National Sceince Foundation (NSF 1840842).

Author Contributions: Z.C., I.N.P., and J.Z. designed the research, analyzed the data and wrote the manuscript. F.Z., S.W., Yan.L., J.W., C.Z., Y.Y., and L.H. performed the experiments, analyzed the data and draft the manuscript. Y.W. provided the technical support and analyzed the data. Yong.L., and B.Y. interpreted data. All authors contributed to data interpretation and commented on the manuscript.

Conflicts of Interest: Authors declare no conflict of interest.

Declaration of transparency and scientific rigour

This Declaration acknowledges that this paper adheres to the principles for transparent reporting and scientific rigour of preclinical research as stated in the BJP guidelines for Design and Analysis, and Animal Experimentation, and as recommended by funding agencies, publishers and other organisations engaged with supporting research.

Data and materials availability: All data needed to evaluate the conclusions in the paper are present in the paper and/or the Supplementary Materials. Additional data related to this paper may be requested from the authors.*AITC*, allyl isothiocyanate

2-APB, 2-aminoethoxydiphenyl borate

AUC, area under the curve

BSA, bovine serum albumin

CMEA, cocamide monoethanolamide

DMEM, Dulbecco's modified eagle medium

DMSO, dimethyl sulfoxide

eYFP, enhanced yellow fluorescence protein

FBS, fetal bovine serum

FLIPR, fluorescent imaging plate reader

G418, geneticin

GFP, green fluorescence protein

HEK-293, human embryonic kidney 293

HEPES, 4-(2-hydroxyethyl)-1-piperazineethanesulfonic acid

KO, knockout

LAMEA, lauric acid monoethanolamide

NGF, nerve growth factor

TRPV1, transient receptor potential vanilloid subtype 1

PDL, poly-D-lysine

RP-HPLC, reverse-phase high performance liquid chromatography

TG, trigeminal ganglion

TRP, transient receptor potential

WT, wild type

Abstract

Background and Purpose: Cocamide monoethanolamide (CMEA) is commonly used as a surfactant-foam booster in cosmetic formulations. Upon contact with the eye or other sensitive skin areas, CMEA elicits sting and lasting irritation. We hypothesized a specific molecular interaction with TRPV1 by which CMEA caused eye irritation.

Experimental Approach: Eye irritancy is evaluated using eye-wiping test in rabbit and mouse. Intracellular Ca^{2+} concentrations and action potentials are measured using Ca^{2+} imaging and current clamp, respectively. Voltage clamp, site-direct mutagenesis and molecular modeling identify the binding pocket of CMEA on TRPV1.

Key Results: CMEA-induced eye irritation is ameliorated by selective ablation of TRPV1 and rodents exhibit much stronger responses to CMEA than rabbits. In trigeminal ganglion neurons, CMEA induces Ca^{2+} influx and neuronal excitability, effects mitigated by TRPV1 inhibitor and absent in TRPV1 knockout neurons. In HEK-293 cell expressing TRPV1, CMEA increases whole-cell currents by increasing channel open probability (EC_{50} = 10.2 μM) without affecting TRPV2, 3, 4 and TRPA1 activities. Lauric acid monoethanolamide (LAMEA), the most abundant constituent in CMEA, is the most efficacious and potent TRPV1 activator. LAMEA binds to the capsaicin-binding pocket of TRPV1. Both rabbit TRPV1 that possesses the T550I variant and the human $TRPV1^{T550I}$ mutant exhibit much lower sensitivity to LAMEA.

Conclusions and Implication: CMEA directly activates TRPV1 to produce eye irritation, and rabbit, the traditional animal model used for eye irritancy test is a poor model for evaluating human eye irritants structurally related to CMEA. Our study identifies potential alternatives to CMEA as non-irritating surfactants.

Key words

cocamide monoethanolamide, eye irritant, transient receptor potential vanilloid type 1

Bullet point summary:

What is already know

- CMEA cause eye and skin irritation

What this study adds

- CMEA-induced irritation is through direct activation of TRPV1 by binding to capsaicin binding pocket
- Rabbit TRPV1 that possesses the T550I variant is less sensitive to CMEA

Clinical significance

- Rabbit is a poor model for evaluation human eye irritants structurally related to CMEA
- This study identifies potential alternatives to CMEA as non-irritating surfactant

Introduction

A major concern of cosmetic formulation is safety. Cosmetic formulations (such as shampoo) induce enduring eye irritation with inadvertent contact with the eyes. Ingredients in cosmetic products are routinely tested for toxicity and other adverse outcomes using animal models, however, with standards much less stringent than those used for active principles in drugs (Monnot *et al.*, 2019). Cocamide monoethanolamide (CMEA, CAS No. 68140-00-1, average MW: 261) is a mixture of ethanolamines of fatty acids hydrolyzed from coconut oil, in which the major constituents are saturated triglycerides such as trimyristin, trilaurin, tripalmitin and tristearin (Wenninger *et al.*, 1997). CMEA is a well-known ocular irritant, although its biological target(s) for eliciting physiological pain responses remains unknown. Instilling CMEA into the conjunctival sac of rabbit induces discomfort of the eye,

conjunctival irritation and slight corneal clouding (Belsito *et al.*, 2012). Nonetheless, CMEA remains an effective and cheap surfactant-foam booster and viscosity enhancer widely used in cosmetic formulations including shampoos, bath oils, shaving creams, soaps, etc. (Wenninger *et al.*, 1997). The prevalent concentrations of CMEA in cosmetic formulations ranges from 1-5 % (38 mM -191 mM) (Belsito *et al.*, 2012). According to the report from FDA, CMEA is used in 294 cosmetic formulations (Lanigan *et al.,* 1999), including most major brands on the market.

Eye irritation is largely related to activation of nociceptors (Garle *et al.*, 2003). Transient receptor potential vanilloid type 1 (TRPV1) ion channel is a well-characterized nonselective cation channels (Julius, 2013). It can be activated by multiple physical and chemical stimuli including noxious heat (> 40 °C), pungent chemicals, protons and animal toxins (Arpad *et al.*, 2007). Activation of TRPV1 leads to a burning sensation, whereas TRPV1-deficient mice show reduced pain responses to defined stimuli (Julius, 2013). TRPV1 channels are predominately expressed in small diameter sensory C-fiber and Aδ polymodal nociceptors (Palazzo *et al.*, 2012). The cornea and mucosal tissue in conjunctiva is densely innervated by sensory afferent nerve fibers that originate from the ophthalmic or medial branch of the trigeminal ganglion (Müller *et al.*, 2003). A large population of corneal small diameter neurons are TRPV1-immunopositive and are highly sensitive to capsaicin in electrophysiological tests (Liu *et al.*, 2003; Nakamura *et al.*, 2007; Leijon *et al.*, 2019). In addition, TRPV1 is also expressed in a variety of skin cells, including epidermal keratinocytes, mast cells, Langerhans cells, and sebocytes (Ho *et al.*, 2015). Activation of TRPV1 in human epidermal keratinocytes releases a variety of pro-inflammatory cytokines

which sensitize nociceptors thereby initiating sensation of pain (Sipos *et al.*, 2005). Previous studies have shown that formulations contain CMEA or anionic linear aliphatic surfactants induced Ca^{2+} influx in neuroblastoma SH-SY5Y cells stably expressing TRPV1 (Lindegren *et al.*, 2009; Forsby *et al.*, 2012). These data raise the hypothesis that activation of TRPV1 ion channels is a major molecular mechanism responsible for eye irritation of some cosmetic formulations (Forsby *et al.*, 2012).

Materials and Methods

Materials

CMEA (coconut monoethanol amide) was purchased from Usolf Chemical Technology Co. Ltd (Qingdao, Shandong, China). SB-366791, capsaicin, and GSK1016790A were purchased from Tocris Bioscience (Bristol, United Kingdom). Allyl isothiocyanate (AITC), cinnamaldehyde, 2-aminoethoxydiphenyl borate (2-APB), 4-(2-hydroxyethyl)-1-piperazineethanesulfonic acid (HEPES), Dulbecco's Modified Eagle Medium (DMEM), bovine serum albumin (BSA), soybean trypsin inhibitor, collagenase A, nerve growth factor (NGF), hygromycin, poly-D-lysine (PDL), and 2-hydroxyethyl laurate (compound **8**) were purchased from Sigma-Aldrich (St. Louis, MO, USA). Fluo-4/AM was purchased from AAT Bioquest (Sunnyvale, CA, USA). Penicillin and streptomycin, geneticin (G418), blasticidin, trypsin, fetal bovine serum (FBS), and lipofectamine® 2000 were purchased from ThermoFisher Scientific (Waltham, MA, USA). All the inorganic chemicals were from Sigma-Aldrich unless indicated. HEK-293 cells (CLS Cat# 300192/p777_HEK293, RRID:CVCL_0045) stably expressing mTRPV2, mTRPV3, hTRPV4 or hTRPA1 were generous gifts from Prof. Michael X. Zhu from University of Texas Health Science Center at Houston.

Isolation and structure determination of CMEA

CMEA was subjected to a semi-preparative reverse-phase high performance liquid chromatography (RP-HPLC) on an Ultimate XB-C18 column (9.2 × 250 mm, Welch Materials Inc., Shanghai, China) in an Agilent 1260 Infinity system (Agilent Technologies, Santa Clara, CA, RRID: SCR_019348). The column was eluted with 5% methanol for 5 min followed by a gradient concentration of methanol from 5% to 100% over 50 min at a flow rate of 2 mL min^{-1}. Seven main peaks (Compounds **1-7, Figure S2A**) detected at 220 nm were collected and their structures were determined by NMR spectroscopic data as described in **Supplemental file**. The relative abundance of these compounds was calculated according to their relative peak absorption at 220 nm. The molecular weight of CMEA was calculated to be 261.36 g/mol based on the percentage and molecular weight of each monomer.

Synthesis of N-(2-sulfanylethyl)dodecanamide (9), N-(2-aminoethyl)dodecan- amide (10) and N-propyllauroylamide (11)

N-(2-sulfanylethyl)dodecanamide (CAS:6162-66-9) (Compound **9**) was synthesized by mixing laurel chloride (1.00 g) and 2-mercaptoehylamine (0.39 g) in a dichloromethane (20 mL) solvent containing triethylamine (0.51 g). After reacting at 0 °C for 30 min, the mixture was stirred at RT for an additional 5 h and a volume of 5 mL 2N hydrochloride acid was added. The residue was purified by silica gel column chromatography to afford compound **9** (1.10 g, 95%) as white solid. The structure was confirmed to be N-(2-sulfanylethyl)dodecanamide by ^{1}H-NMR, ^{13}C-NMR, and mass spectrum.

N-(2-aminoethyl)dodecanamide (CAS:10138-02-0) (Compound **10**) was synthesized by mixing laurel chloride (1.00 g) with N-boc-ethylenediamine (0.80 g) in a dichloromethane solvent (20 mL) containing triethylamine (0.51 g) for 30 min at 0 °C. The resulting mixture was then stirred at room temperature for 3 h and the reaction products were filtered, and the residue was suspended in a 20 mL dichloromethane and a volume of 7 mL of trifluoroacetic

acid was added. The solution was stirred at room temperature for 3 h and the reaction products were applied into the silica gel column chromatography to afford compound **10** (0.83 g, 75%) as white solid. The structure was confirmed to be N-(2-aminoethyl)dodecanamide by ^{1}H-NMR, ^{13}C-NMR, and mass spectrum.

N-propyllauroylamide (CAS:110790-31-3) (Compound **11**) was synthesized by mixing laurel chloride (1.00 g) with propylamine (0.30 g) in a dichloromethane (20 mL) solvent containing triethylamine (0.51 g). After reaction for 30 min at 0 °C, the mixture was stirred for an additional 3 h and a volume of 5 mL 2 M hydrochloride acid was added. The residue was purified by silica gel column chromatography to afford compound **11** (1.05g, 95%) as white solid. The structure was confirmed to be N-propyllauroylamide by ^{1}H-NMR, ^{13}C-NMR, and mass spectrum.

Animals

All animal experiments were carried out in accordance with the National Institutes of Health guide for the care and use of Laboratory animals (NIH Publications No. 8023, revised 1978) approved by the China Pharmaceutical University Institutional Animal Care and Use Committee (#SYXK 2016-0011). The study was designed to generate groups of equal size and NC3Rs (National Center for Replacement, Refinement and Reduction of Animals) principles were taken into consideration for the sample sizes of animal experiments using randomization and blinded analysis (Kilkenny *et al.*, 2010; McGrath *et al.*, 2015). Animal studies were in compliance with the ARRIVE guidelines (Kilkenny *et al.*, 2010; Curtis *et al.*, 2015; McGrath *et al.*, 2015; Lilley *et al.*, 2020). The number of animals and group sizes were calculated based on our previous experience (Wang *et al.*, 2021). Animals were treated humanely and with regard for alleviation of suffering. Sixty four C57BL/6J mice (6-8 wk old male and female with 1:1 ratio at 18-22 g, n = 8/group) and sixty four albino New Zealand rabbits (35 wk old male and female with 1:1 ratio at ~ 4.0 kg, n = 8/group) were purchased

from QingLongShan Laboratory Animal Center (Nanjing, Jiangsu, China). Six to eight wk old male and female (1:1) TRPV1 knockout (KO) C57BL/6J mice (B6.129X1-Trpv1^{tm1Jul}/J, Stock No: 003770, the Jackson Laboratory, RRID: IMSR_JAX:003770, n = 32 mice, n = 8/group) were from Prof. Yong Li at Shanghai Jiao Tong University (Shanghai, China). All the animals were maintained in a temperature-controlled (23 ± 2 °C) vivarium at a 12-h light/dark cycle provided with food and water *ad libitum*.

Eye irritation test

The eye-wiping test was used to evaluate the eye irritation of CMEA in mouse or rabbit as described previously (Iwasaki *et al.*, 2006). CMEA solutions (4, 10, 20, or 40 mM dissolved in 0.9% NaCl + 1% DMSO) were instilled into the eyes of mouse (10 μL eye^{-1}) or rabbit (100 μL eye^{-1}) using micropipette. AITC (10 mM) and capsaicin (1 mM) were used as positive controls. To test the role of TRPV1 on the CMEA eye irritation, the TRPV1 inhibitor SB-366791 (17 mM) was administrated into the mouse or rabbit eyes simultaneously with CMEA. The eye-wiping numbers were manually counted for an epoch of 1 min right after drug administration. The drugs were prepared and administrated with the investigator blinded to treatment. Euthanasia was performed by CO_2 inhalation after eye irritation tests.

Acute isolation of trigeminal ganglion neurons

Trigeminal ganglion (TG) neurons were isolated from wild type (WT) or TRPV1 KO mice as described previously (Katzenell *et al.*, 2017). Briefly, after CO_2 asphyxiation, mice were decapitated, and the trigeminal ganglions were dissected. The collected trigeminal ganglions were incubated with 0.05% trypsin and 0.03% collagenase A for 25 min at 37 °C. The dissociated TG neurons were resuspended in DMEM medium supplemented with 10% FBS, 1% GlutaMAX, 50 ng mL^{-1} NGF, 1% HEPES and 100 U mL^{-1} penicillin, 100 μg mL^{-1} streptomycin and plated onto PDL (50 μg mL^{-1}) pre-coated 96-well plates for Ca^{2+} imaging or 35-mm petri-dishes for current clamp recordings respectively. The neurons were cultured in

an incubator with 95% humidity and 5% CO_2 at 37 °C for 6 h before experiments.

Calcium imaging

Calcium imaging was performed as described previously (Cao *et al.*, 2013). After aspirating the medium, TG neurons were incubated with Fluo-4/AM (4 μM) in Locke's buffer (in mM: 8.6 HEPES, 5.6 KCl, 154 NaCl, 5.6 glucose, 1.0 $MgCl_2$, 2.3 $CaCl_2$, and 0.1 glycine, pH 7.4) containing 5 mg mL^{-1} BSA for 60 min at 37 °C. The images were continuously digitized at a sampling rate of 1 frame s^{-1} using a Flash4.0 V2 digital CMOS camera (Hamamatsu Photonics, Iwata, Shizuoka) in a Leica DMi8 microscope (Leica Microsystems, Wetzlar, Germany) under FITC fluorescent channel controlled by Leica Application Suite X (LAS X) software (Leica Microsystems, RRID: SCR_013673). The Fluo-4 arbitrary fluorescent unit of each cell (ROI, region of interest) was analyzed using LAS X software (Leica Microsystems). Compounds were introduced by bulk perfusion at a flow rate of 2 mL min^{-1}. Data were presented as F/F_0 where F is the fluorescent signal at different time points, whereas F_0 is the average value of the initial five data points.

Molecular cloning and transient transfection

Rabbit TRPV1 (oTRPV1) cDNA construct was synthesized by GenScript Biological Technology Co., Ltd. (GenScript, Nanjing, China) and validated by sequencing. To facilitate identification of hTRPV1 and oTRPV1 transfected cells, enhanced yellow fluorescence protein (eYFP) was genetically linked to the C terminus of hTRPV1 and a cDNA construct encoding green fluorescence protein (GFP) was co-transfected with oTRPV1 plasmid, respectively. Point mutations were generated using KOD plus mutagenesis kit (Toyobo, Osaka, Japan). All mutants were confirmed by DNA sequencing.

HEK-293 cells were maintained in DMEM medium supplemented with 10% FBS, penicillin and streptomycin. Cells were transiently transfected with cDNA constructs by lipofectamine® 2000 according to the manufacturer's protocol. Patch-clamp recordings were

performed after 24 – 48 h transfection.

Intracellular Ca^{2+} determination

Intracellular Ca^{2+} concentration was determined as described previously (Zhou *et al.*, 2018). Briefly, after incubation with Fluo-4/AM (4 μM) for 60 min at 37 ºC, HEK-293 cells expressing hTRPV1, mTRPV2, mTRPV3, hTRPV4 or hTRPA1 were gently washed four times and loaded into the chamber of a fluorescent imaging plate reader (FLIPR$^{TETRA®}$; Molecular Devices, Sunnyvale, CA, USA) with temperature set at 37 °C for hTRPV1, mTRPV2, hTRPA1, and 25 °C mTRPV3 and hTRPV4. Cells were excited at 470-495 nm and the emission at 515-575 nm was recorded at 1 s intervals. After recording the baseline fluorescence (F_0) for around 60 s, different concentrations of CMEA (final concentrations, 0.4-40 μM) were added by an automated, programmable pipetting system, and the fluorescent signals (F) were recorded. To examine whether CMEA had an inhibitory effect on mTRPV2, mTRPV3, hTRPV4 or hTRPA1, a second addition of respective agonist was introduced on 180 s to stimulate Ca^{2+} response. The agonists used were 2-APB (300 μM) for mTRPV2 and mTRPV3, GSK106790A (30 nM) for hTRPV4, and cinnamic aldehyde (300 μM) for hTRPA1. Data were presented as F/F_0. To analyze the concentration-response relationship for CMEA activation of hTRPV1, the area under the curve (AUC) was calculated from a time period of 300 s right after the addition of CMEA.

Electrophysiology

All the electrophysiological experiments were performed using EPC-10 amplifier (HEKA Instrumental Inc. Holliston, MA, USA, RRID: SCR_014270) driven by PatchMaster software (HEKA, RRID: SCR_000034) at room temperature (~24 °C). Pipettes were pulled from 1.5-mm capillary tubing using a horizontal micropipette puller (P-1000, Sutter Instrument Company, Novato, CA) with tip resistance of 2-3 MΩ and 8-10 MΩ for whole-cell and outside-out recording, respectively. Small (< 30 μm) or medium (30-50 μm)

diameter TG neurons were used to record action potentials using current-clamp described previously (Zhao *et al.*, 2019). The pipette solution contained (in mM): KCl 140, $MgCl_2$ 5, $CaCl_2$ 2.5, EGTA 5, ATP 4, GTP 0.3, and HEPES 10 (pH adjusted to 7.3 with KOH). The external solution contained (in mM): NaCl 140, $MgCl_2$ 1, KCl 5, $CaCl_2$ 2, glucose 10, and HEPES 10 (pH adjusted to 7.3 with NaOH). The action potentials were evoked by a 100-pA depolarization current with a duration of 1 s and the stimulations were repeated every 15 s.

Whole-cell TRPV1 currents were recorded as described previously (Yin *et al.*, 2013). Cells were bathed in external solution containing (in mM): NaCl 140, KCl 5, $MgCl_2$ 1, glucose 10, and HEPES 10 (pH adjusted to 7.2 with NaOH). Pipette solution contained (in mM): CsCl 140, $MgCl_2$ 1, EGTA 5, $CaCl_2$ 0.1, and HEPES 10 (pH adjusted to 7.2 with CsOH) (Hu *et al.*, 2006). Serial resistance was compensated by 80%. Cells were held at 0 mV and voltage ramps (100 ms) from −100 to +100 mV were applied every 1 s. The resulting currents were recorded at 10 kHz. Drugs diluted in the bath solution was applied through a press-driven multichannel system (ALA scientific instruments, Farmingdale, NY) with the outlet placed approximately 50 μm away from the recording cell or membrane.

Single-channel recording was performed under outside-out configuration at holding potential of +80 mV. Single channel currents were acquired at 10 kHz, and then filtered with 2 kHz low pass filter. Analysis were performed using Clampfit 10.4 software (Molecular Devices, California, USA, RRID: 011323) for to calculate the open probability (P_o) of hTRPV1 channels.

Metadynamics

As previously described, during metadynamics simulations, an iterative process of chosen collective variables (CV) are modified by adding the repulsive potential of Gaussian shape at precise locations of ligand-binding site (Laio *et al.*, 2008). DESMOND (RRID: SCR_014575) (Wang *et al.*, 2018) was used to analyze potential CMEA binding sites with a

constant number of particles, pressure (1 bar), temperature (300 ^{o}K) (NPT) and periodic boundary conditions (PBC) using Nose-hoover chain Thermostat and Martyna-Tobias-Klein Barostat methods. All-atom OPLS_2005 force field for proteins, ions, lipids and the simple point charge for water were used in all simulations. The parameters for height and width of the Gaussian and the interval were set to 0.12 kcal mol^{-1}, 0.05 Å and 0.09 ps, respectively. Cryo-EM structure of TRPV1 (PDB code: 3J5R) with a compound **3** (lauric acid monoethanolamide) aligned to the binding site of capsaicin was set to the initial model in the simulations. DELL T7910 graphic working station (with NVIDIA Tesla K40C-GPU) was used to run the metadynamics simulations and a 12-CPU CORE DELL T7500 graphic working station was used to perform preparation, analysis and visualization. Metadynamics Analysis Tools in the DESMOND (Shaw, 2005) were used to generate the sum of the Gaussians and the free-energy surface.

Data analysis

The data and statistical analysis were complied with the recommendations of the British Journal of Pharmacology on experimental design and analysis in pharmacology (Curtis *et al.*, 2018). The unequal group sizes in the cells carrying TRPV1 mutant were because the recordings of some transfected cells were not successful. Declared group sizes represented the number of independent values (one data point per animal or cell) and all statistical analyses were performed using such independent values (technical replicates were not considered independent values). Statistical analysis was undertaken only for studies where each group size was at least n = 5. No data points were excluded from the analysis in any results. For experiments with a smaller sample size (that is, n < 5), data were presented as preliminary observations and were not subjected to statistical analysis in this study.

In WT-hTRPV1 channels, the currents induced by CMEA or compound **1-11** were normalized to capsaicin (1 μM) in respective cell. The response of compound **3** in hTRPV1 mutants, oTRPV1 and oTRPV1 mutants were all normalized to that of 2-APB (3 mM) in respective cell. Data gained were graphed using Prism Graph Pad 7.0 software (GraphPad Software Inc., San Diego, CA, USA, RRID: SCR_002798) or Origin 8.0 (OriginLab, Massachusetts, USA, RRID: SCR_002815). Y axis is labelling in figures using 'fold matched control values'. Each data point represents the Mean ± SEM. Concentration-response relationship curves were analyzed by nonlinear regression analysis using Prism Graph Pad 7.0 software (GraphPad Software Inc.). Statistical significance between groups was calculated using one-way ANOVA; and only if F in ANOVA achieved *P* value less than 0.05, a *post hoc* Bonferroni comparison was conducted. *P* values below 0.05 were considered to be statistically significant. All data were tested for normal distribution and equal variance.

Nomenclature of Targets and Ligands

Key protein targets and ligands in this article are hyperlinked to corresponding entries in http://www.guidetopharmacology.org/, the common portal for data from the IUPHAR/BPS Guide to PHARMACOLOGY (Harding *et al.*, 2018), and are permanently archived in the Concise Guide to PHARMACOLOGY 2019/20 (Alexander *et al.*, 2019).

Results

TRPV1 mediates CMEA-induced ocular irritation

The typical species used for testing eye irritancy of cosmetic formulations has been the rabbit *in vivo* model (Holden, 1989). Instillation of vehicle (0.9% NaCl + 1% DMSO, 100 μL/eye) to the rabbit eye had no effect (**Fig. 1A**) whereas local administration of a TRPA1 activator, allyl isothiocyanate (AITC, 10 mM, 100 μL eye^{-1}) or the TRPV1 activator, capsaicin (1 mM, 100 μL eye^{-1}) induced strong eye-wiping behaviors at a frequency of 21.3 ± 1.4 min^{-1} (n = 8 rabbits, $P < 0.05$) or 12.3 ± 1.2 min^{-1} (n = 8 rabbits, $P < 0.05$), respectively. Instillation of CMEA (4-40 mM, 100 μL eye^{-1}) induced a dose-dependent eye-wiping response in rabbit whose magnitude at the maximum dose (1 mg/eye) tested was 7.5 ± 1.3 min^{-1} (n = 8 rabbits, $P < 0.05$ *vs.* vehicle), only 35% of that observed with AITC (**Fig. 1A**). Co-administration of a TRPV1 selective inhibitor SB-366791 (Varga *et al.*, 2005) (17 mM, 100 μL eye^{-1}) reduced the frequency of CMEA-induced eye-wiping from 7.5 ± 1.3 min^{-1} to 3.1 ± 1.0 min^{-1} (n = 8 rabbits, $P < 0.05$) (**Fig. 1A**), indicating a role of TRPV1 in mediating CMEA-induced eye irritation. Noticeably, CMEA (and capsaicin) but not AITC induced stronger eye-wiping behaviors in mice than rabbits that could also be markedly attenuated by SB-366791 (**Fig. 1B**). Importantly, TRPV1 knock out (KO) mice did not respond to either CMEA or capsaicin, whereas AITC elicited eye-wiping behaviors that were comparable to wildtype (WT) mice (**Fig. 1C**). These observations suggest that CMEA is a strong eye irritant likely through the TRPV1 pathway, and rabbits are a less responsive model for irritancy testing with CMEA and possibly its analogs.

CMEA induces Ca^{2+} influx and action potential firing in acutely isolated trigeminal ganglion neurons of wildtype but not TRPV1 KO mice

TRPV1 is a Ca^{2+}-permeable channel abundantly expressed in trigeminal ganglion (TG) neurons. We found that brief exposure of capsaicin (1 μM), CMEA (40 μM) and AITC (100

μM) induced a rapid and robust Ca^{2+} influx in TG neurons loaded with Fluo-4/AM (**Fig. 2A**). Among 415 TG neurons recorded that responded to KCl depolarization, 187 (45%) and 66 (16%) neurons responded to capsaicin (Cap^{+}) and AITC ($AITC^{+}$), respectively (**Fig. 2B**). A small portion of TG neurons (5.7%) responded to both capsaicin and AITC exposure (**Fig. 2B**). Over 60% of capsaicin-responsive TG neurons responded to CMEA (**Fig. 2B**), consistent with pharmacological responses with animal tests (**Fig. 1B**). TRPV1 inhibitor SB-366791 completely suppressed CMEA-induced Ca^{2+} elevation in capsaicin-responsive TG neurons (**Fig. 2C**). Although a fraction of TRPV1 KO TG neurons responded to AITC exposure, none of them responded to CMEA or capsaicin (**Fig. 2D**).

We next investigated whether CMEA was capable of affecting action potential (AP) firing in TG neurons. TRPV1 channels are mainly expressed in small (< 30 μm) and medium-diameter (30-50 μm) nociceptive sensory neurons, whereas less than 3% of the large-diameter (> 50 μm) TG neurons express TRPV1 (Shimizu *et al.*, 2007). We therefore recorded membrane potential and action potential firing with and without CMEA exposure in small- and medium-diameter TG neurons obtained from both WT and KO mice. In WT TG neurons, application of CMEA resulted in a concentration dependent depolarization of the membrane potential; however, no change in membrane potential was observed in KO TG neurons in the presence of CMEA (**Fig. 2E**). Furthermore, CMEA at concentration of 0.4 μM significantly increased the frequency of tonic-spiking in WT TG neurons induced by a 100-pA current injection (1 s), whereas ≥ 1.2 μM CMEA suppressed the tonic-spiking firing (**Fig. 2F & H**). Although KO neurons yielded similar AP firing patterns in response to current injection (100 pA), they were not affected by CMEA (**Fig. 2G-H**). These data demonstrate TRPV1-dependent neuronal activation by CMEA. The bidirectional response in the AP firing

of CMEA is likely dependent on the membrane depolarization. The small depolarization of membrane potential can facilitate the AP firing. However, when the membrane potential depolarized to $\geqslant$ –40 mV, most of voltage-gated sodium channels will get into inactivated state leading to depolarization dependent blockade of AP. This is also consistent with previous report where capsaicin induced bidirectional response on the action potential firing (Urban *et al.*, 1993; Wu *et al.*, 2013).

CMEA directly activates TRPV1

Given the role of TRPV1 in CMEA-induced eye irritation as well as CMEA effects on Ca^{2+} influx and action potential firing in TG neurons, we next investigated the direct effects of CMEA on hTRPV1. HEK-293 cells expressing hTRPV1 responded to capsaicin (1 μM) with a rapid cation current that was markedly outwardly rectified. Likewise, CMEA elicited similar rectified currents with an EC_{50} value of 10.2 μM (**Fig. 3A & B**). The maximal current response at +100 mV was 62.4% of that induced by 1 μM capsaicin (**Fig. 3C**), indicating strong TRPV1 activation by CMEA. Application of SB-366791 completely abolished CMEA-induced TRPV1 current (**Fig. 3A-C**). Single-channel recordings at +80 mV revealed that CMEA directly increased hTRPV1 channel activity by increasing channel open probability (P_o) from 0.004 ± 0.008 to 0.387 ± 0.027 (n = 6 cells, $P < 0.05$), and the effect was completely abolished by SB-366791 (P_o = 0.017 ± 0.007, $P < 0.05$ *vs.* CMEA; $P = 0.13$ *vs.* vehicle control, n = 6 cells) (**Fig. 3D-F**).

Many cosmetic products were formulated to be weakly acidic (Tarun *et al.*, 2014). Since TRPV1 activity can be strongly potentiated by proton concentration, we examined the effect of CMEA at physiological extracellular pH (7.4) and pH 6.5. CMEA at 4.0 μM had little effect on hTRPV1 at pH 7.4, whereas CMEA enhanced acidification (pH 6.5)-induced current from 49.0± 3.4% to 77.5 ± 10.3% ($P < 0.05$, n = 5 cells) of capsaicin (1 μM) response

at pH 7.4 (**Fig. 3G-I**).

To further evaluate the specificity of these effects, we tested CMEA on HEK-293 cells that expressed TRPV1 orthologs, TRPV2, 3 and 4. Application of CMEA (120 µM) had no effect on the 2-APB-induced Ca^{2+} responses in HEK-293 cells expressing either mTRPV2 or mTRPV3 channels (**Fig. S1A & B**). Similarly, CMEA was ineffective on GSK1016790A-induced Ca^{2+} influx in hTRPV4-transfected HEK-293 cells (**Fig. S1C**). Many irritants such as tear gas, mustard oil, nicotine, and cinnamaldehyde activate TRPA1 receptors (Gijsen *et al.*, 2010). However, CMEA (120 µM) had no effect on TRPA1-mediated Ca^{2+} influx induced by cinnamaldehyde (**Fig. S1D**).

Lauric acid monoethanolamide (3) is the most effective CMEA compound in activating hTRPV1

CMEA is a mixture of ethanolamines of fatty acids. We separated the chemical constituents of CMEA using RP-HPLC. A total of seven peaks were resolved and isolated (**Fig. S2A**). Their chemical structures were determined based on NMR and MS spectra (**Fig. 4A, see also supplementary file**). These compounds shared common features including a hydroxyl group (termed the head), an acylamide group (termed the neck) and an aliphatic chain with varying numbers of carbon atoms and unsaturation (termed the tail) (**Fig. 4A**). The relative abundance of these compounds in CMEA is shown in **Figure S2B**; compound **3** (lauric acid monoethanolamide) was the most abundant component, accounting for 46.3% of CMEA (**Fig. S2B**). We tested each CMEA constituent on hTRPV1 and found that, at 30 µM, compounds **2-7** but not compound **1** elicited hTRPV1 currents that were abolished by SB-366791 (**Fig. 4B**). Analysis of the concentration-response relationships showed that the EC_{50} of compounds **2-7** for TRPV1 activation were similar, ranging from 3.20 µM (compound **3**) to 6.74 µM (compound **4**) (**Figure S2B**). The rank order of efficacy to activate TRPV1 was **3 > 5 ≈ 7 > 4 > 6 > 2** (**Figure S2B**). Compound **3** containing a C_{11} tail was

most efficacious. Increasing or decreasing the tail length from C_{11} gradually decreased efficacy (**Fig. 4A; Figure S2B**). Importantly, efficacy toward hTRPV1 does not correlate with partition coefficient (Log P) and therefore solubility of these compounds (**Fig. S2B**).

Structural determinants of compound 3

Considering compound **3** was the most efficacious and most abundant constituent of CMEA, we designed a series of derivatives based on compound **3** to further investigate structural determinants important for interactions with hTRPV1. The functional contribution of the neck acylamide group was assessed by substituting an ester linkage to yield compound **8** (**Fig. 4E**). As shown in **Figure 4F**, compound **8** at concentration up to 100 μM had negligible activity on hTRPV1, confirming the importance of the acylamide group reminiscent of results previously published with modifications of acylamide group of capsaicin (Yang *et al.*, 2015). Substitution of the compound **3** hydroxyl to -SH (**9**), $-NH_2$ (**10**), or $-CH_3$ (**11**), largely eliminated activity toward hTRPV1 (**Fig. 4F**). These results suggest that both the head and neck of the CMEA compounds are required for interacting with hTRPV1.

Compound 3 activates hTRPV1 through binding to the vanilloid binding pocket

Results shown in **Figure 4E & F** indicated that compound **3** and its analogs might mimic capsaicin when bound to hTRPV1, forming specific interactions with their head and neck groups. Capsaicin interact with TRPV1 with two critical hydrogen bonds, one between the neck amide of capsaicin and the hydroxyl group of T551 in the S4 segment of mouse TRPV1, the other between the head hydroxyl group of capsaicin and the carboxyl group of E571 within the S4-S5 linker (Yang *et al.*, 2015; Yang *et al.*, 2017). CMEA compounds contain the same neck amide group as capsaicin. We found that, when T550 in hTRPV1 (equivalent to T551 of mTRPV1) was mutated to an isoleucine, the channel's sensitivity to compound **3** decreased ~5 folds (**Fig. 5A & B; Table S1**). Interestingly, T550 is highly conserved in all highly capsaicin-sensitive TRPV1 channels (e.g., human, mouse, rat).

However, rabbit expresses the T550I TRPV1 variant, which has been shown to be significantly less responsive to capsaicin (Gavva *et al.*, 2004). Indeed, oTRPV1 exhibited a low sensitivity to compound **3** consistent with results with hTRPV1^{T550I}, whereas expression of the I550T substitution in oTRPV1 yielded a highly sensitive channel (**Fig. 5A & B; Table S1**).

The key residue interacting with capsaicin's head, E570 (equivalent to E571 in mTRPV1), is also critical for hTRPV1 activity toward compound **3**. The E570A mutant failed to respond to compound **3,** even at 100 μM, though the mutant retained a robust response to 2-APB (**Fig. 5C & D**). Sequence alignment of S3, S4 and the adjacent regions revealed that there are five additional divergent amino acid residues between hTRPV1 and oTRPV1 (**Fig. S3**). Each of these residues in hTRPV1 was mutated to the corresponding residue in oTRPV1 (yielding hTRPV1^{T505A}, hTRPV1^{L518V}, hTRPV1^{S520A}, hTRPV1^{L534C}, and hTRPV1^{S540T}). None of the mutants when expressed in HEK-293 exhibited significant changes in response to compound **3** (**Table S1**). On the other hand, mutations to residues known to be critical for capsaicin activation (Gavva *et al.*, 2004) substantially reduced compound **3** activation (**Fig. 5C & D**), suggesting that compound **3** interacts with hTRPV1 with molecular determinants similar to those of capsaicin (Yang *et al.*, 2015; Yang *et al.*, 2017).

Computational modeling of compound 3 binding to hTRPV1

To further understand molecular determinants responsible for CMEA interactions with hTRPV1, we used metadynamics simulations. Since no three-dimensional structure of hTRPV1 is currently available, the cryo-EM structure of rat TRPV1 (rTRPV1, 85.83% sequence identity) was used as the template. The distance between the oxygen atom on the head group of compound **3** and the C_β of E570 (rTRPV1 numbering), and the dihedral angle of compound **3** were defined as two different variables, CV1 and CV2. With these definitions, compound **3**/rTRPV1 interaction modes with the lowest binding free energies were calculated

and compared. Based on the reconstructed free energy surface (FES), we identified the best mode with the lowest binding free energy, named IM1 (**Fig. 5E**). In IM1, the head and neck groups of compound **3** make hydrogen bond (H-bond) contacts with three residues of rTRPV1, including E570, Y511 and T550 (**Fig. 5E & F**). The long aliphatic chain of compound **3** forms hydrophobic interactions with residues from two neighboring subunits that form the ligand-binding pocket, including F543, A546, A566 and I569 from the S4 transmembrane (TM) domain, and L662, F591, I661, A665 and I 669 from S5&S6 TM domains (**Fig. 5F**).

Model results were consistent with experimental data presented above. Mutations affecting the H-bond formation remarkedly weakened (T550I) or abolished (Y511A, E570A) compound **3**-evoked activation of hTRPV1 (**Fig. 5A-D and Table S1**). Introducing bulkier side chain to residues adjacent to these positions, for example S512Y, also dramatically decreased the apparent affinity and the maximal response of compound **3** (**Fig. 5C & D**) even though S512 was predicted to not directly contact compound **3** in the metadynamics model (**Fig. 5F**). Mutations that were likely to influence hydrophobic contacts with compound **3** in hTRPV1 (**Fig. 5F**), including A566L, F543A, A546L, A566L, I569A, F591A, I661A, I662A and L663A, partially decreased sensitivity of compound **3** in hTRPV1 (**Table S1 and Fig. 5C & D**), especially for A566L (**Fig. 5D**), indicating hydrophobic contacts also contributed to the activities of compound **3**.

We found that compound **3** interacted with the main chain oxygen atom of T550 in the metadynamics mode (**Fig. 5E; Fig. S4**). hTRPV1^{T550I} was 5-fold less sensitive to compound **3** (**Fig. 5A & B**). However, T550A, T550V and T550S mutated hTRPV1 channels showed comparable levels of apparent affinity and maximal efficacy of compound **3** to those of WT hTRPV1 (**Table S1**), suggesting that the side chain of T550 did not make direct contact with compound **3**. The I550 residue in oTRPV1 led to the weak response to compound **3** (**Fig. 5A**

& B; Table S1). Rabbit TRPV1^{I550T} mutant displayed comparable responses to WT hTRPV1 (**Fig. 5A & B; Table S1**). Similarly, I550V, I550A and I550S mutations of oTRPV1 also showed comparable sensitivity to that of WT hTRPV1 (**Table S1**), again suggesting that the main chain atom instead of side chain of T550 in hTRPV1 interacted with compound **3**.

Discussion

The results of the present study provide direct evidence that TRPV1 ion channels are the primary molecular target of CMEA compounds in the eye. Both experimental and molecular simulation modeling define the molecular determinants required for optimizing the binding of CMEA constituents to TRPV1 and this activity fully explains both stinging sensations and subsequent irritation of the ocular system. The activity of CMEA in hTRPV1 is similar to the potency of endovanilloids (Huang *et al.*, 2002; Chu *et al.*, 2003) and within one order of magnitude of the potency exhibited by the exemplary TRPV1 ligand capsaicin (Caterina *et al.*, 1997; Yang *et al.*, 2015). The concentration of CMEA in cosmetic formulations ranges from 0.1% to 25%, with the majority of products containing 1-5% CMEA (Belsito *et al.*, 2012). The wide use of CMEA in cosmetic products at these concentrations facilitates accidental and repeated CMEA exposure to the eye and other sensitive skin areas, as can be attested by daily experiences. Although product labeling warning to avoid direct ocular exposure may have modest impact, the present study identifies a more novel and likely more effective approach to circumventing unwanted effects of CMEA while maintaining desirable surfactant properties in personal hygiene products. Our present study defines the stringent structure-activity relationship of CMEA constituents toward TRPV1 providing leads that decrease target activity and irritancy, while maintaining desirable surfactant properties.

Although the individual constituents identified in CMEA displayed comparable potency, their respective efficacies toward hTRPV1 is strongly dependent on hydrocarbon tail length

and location of unsaturation. This structure-activity profile is consistent with those previously published with capsaicin analogs having variable length of hydrocarbon tail that display distinct sensitivity in activating TRPV1 (Yang *et al.,* 2015). We also demonstrate the importance of the hydroxyl head and acylamide neck of compound **3** that are likely critical contact points within the TRPV1 binding pocket. Arguably the most important aspect of the current structure-activity, is the identity of structural variants of compound **3** that do not activate TRPV1, providing potential alternatives to CMEA as non-irritant surfactants.

Structurally, CMEA is similar to capsaicin having an acylamide neck and hydrocarbon tail with slight difference on the hydroxyl head. We demonstrate that disruption of capsaicin binding domain drastically reduces the sensitivity of compound **3** suggesting that this compound also possibly binds to the capsaicin binding pocket. While the T550I mutant decreases the sensitivity of compound **3**, T550A, T550V and T550S mutants have comparable sensitivity to that of WT hTRPV1 indicating that the main chain atom instead of side chain of T550 of hTRPV1 interacts with this compound. This interaction mode is distinct from that of capsaicin which directly interacts with the oxygen atom of side-chain through an H-bond (Liao *et al.*, 2013; Yang *et al.*, 2015), leading to a ~20-fold decrease in the apparent affinity of capsaicin in $TRPV1^{T550A}$ (Yang *et al.*, 2015). The comparable sensitivity of compound **3** between T550A/V/S and WT is probably because of that the smaller side chain at T550 can be coordinated into the space formed by S4, S5 and S6 TM regions (**Fig. S4B**), consequently having no effect on the sensitivity of compound **3**. When the size became bigger, like T550I (~ 5-fold decrease), the longer side chain cannot be coordinated by this space, thus significantly reducing the sensitivity of compound **3**.

Although oral toxicity of CMEA is low with LD_{50} values of 3.1 g kg^{-1} in mice and 7.2 g kg^{-1} in rat (Belsito *et al.*, 2012), respectively, due to its major use in the cosmetic products, the adverse potential of dermal exposures have been recognized and investigated. CMEA

induces a class 3 reaction (rash) when topically administrated to New Zealand white rabbit for 24 h (Lanigan *et al.*, 1999). A longer exposure of CMEA results in moderate erythema, wrinkling, cracking, dry skin and destructive alternation (necrosis) of the skin tissue (Lanigan *et al.*, 1999). On the basis of the patient history and clinical signs, and the label of the cosmetic products used, CMEA has the potential to induce dermatitis (Mertens *et al.*, 2016). Activation of TRPV1 has been shown to be involved in the skin inflammation (Gouin *et al.*, 2018) and inhibition of TRPV1 represents an attractive target for the treatment of skin inflammatory disease (Aprile *et al.*, 2019). Thus, activation of TRPV1 by CMEA may explain the mechanism of CMEA-induced dermatitis observed in the animal models (Lanigan *et al.*, 1999).

Given the obvious discomfort and potential health concerns associated with CMEA in daily consumer products, why continued wide usage in cosmetic products? Although CMEA use is likely cost-related, an immediately translational outcome of the present study is that at the *in vivo* (rabbit eye irritation assays), as well as cellular and molecular levels, CMEA is much less potent in activating rabbit TRPV1 than human or rodent TRPV1. The difference is due primarily to a single amino acid (T550I variant) substitution within the capsaicin binding pocket of rabbit TRPV1. A similar case has been recently reported in tree shrew that expresses the analogous T to I TRPV1 variant, resulting in the reduced sensitivity to spiciness (Han *et al.*, 2018). Ironically, the standard practice for testing eye irritancy of cosmetic formulations happened to be based on using rabbit as an *in vivo* model (Holden, 1989). We suggest that this practice, established before molecular cloning of TRPV1 as a nociceptor (Caterina *et al.*, 1997), should be reconsidered.

Reference

Alexander SP, Mathie A, Peters JA, Veale EL, Striessnig J, Kelly E, *et al.* (2019). The concise guide to pharmacology 2019/20: Ion channels. *British Journal of Pharmacology* **176:** S142-S228. https://doi.org/10.1111/bph.14749

Aprile S, Serafini M, Pirali T (2019). Soft drugs for dermatological applications: recent trends. *Drug discovery today* **24**(12)**:** 2234-2246. https://doi.org/10.1016/j.drudis.2019.08.007

Arpad S, Cortright D, Blum C, Eid S (2007). The vanilloid receptor TRPV1: 10 years from channel cloning to antagonist proof-of-concept. *Nature Reviews Drug Discovery* **6**(5)**:** 357-372. https://doi.org/10.1038/nrd2280

Belsito M, Hill RA, Klaassen CD, Liebler D, Marks Jr JG, Ronald C (2012). On the Safety Assessment of Ethanolamides as Used in Cosmetics. *Final Amended Report*

Cao Z, Hulsizer S, Cui Y, Pretto DL, Kim KH, Hagerman PJ, *et al.* (2013). Enhanced asynchronous Ca^{2+} oscillations associated with impaired glutamate transport in cortical astrocytes expressing *Fmr1* gene premutation expansion. *Journal of Biological Chemistry* **288**(19)**:** 13831-13841. https://doi.org/10.1074/jbc.M112.441055

Caterina MJ, Schumacher MA, Tominaga M, Rosen TA, Levine JD, Julius D (1997). The capsaicin receptor: a heat-activated ion channel in the pain pathway. *Nature* **389**(6653)**:** 816-824. https://doi.org/10.1038/39807

Chu CJ, Huang SM, Petrocellis LD, Bisogno T, Ewing SA, Miller JD, *et al.* (2003). N-oleoyldopamine, a novel endogenous capsaicin-like lipid that produces hyperalgesia. *Journal of Biological Chemistry* **278**(16)**:** 13633-13639. https://doi.org/10.1074/jbc.M211231200

Curtis MJ, Alexander S, Cirino G, Docherty JR, George CH, Giembycz MA, *et al.* (2018). Experimental design and analysis and their reporting II: updated and simplified guidance for authors and peer reviewers. *British Journal of Pharmacology* **175**(7)**:** 987-993. https://doi.org/10.1111/bph.14153

Curtis MJ, Bond RA, Spina D, Ahluwalia A, Alexander SP, Giembycz MA, *et al.* (2015). Experimental design and analysis and their reporting: new guidance for publication in BJP. *British journal of pharmacology* **172**(14)**:** 3461. https://doi.org/10.1111/bph.12856

Forsby A, Norman K, Andaloussi-Lilja JE, Lundqvist J, Walczak V, Curren R, *et al.* (2012). Using Novel *In Vitro* NociOcular Assay Based on TRPV1 Channel Activation for Prediction of Eye Sting Potential of Baby Shampoos. *Toxicological Sciences* **129**(129)**:** 325-331. https://doi.org/10.1093/toxsci/kfs198

Garle M, Fry J (2003). Sensory nerves, neurogenic inflammation and pain: missing components of alternative irritation strategies? A review and a potential strategy. *Alternatives to Laboratory Animals Atla* **31**(3)**:** 295-316. https://doi.org/10.1177/026119290303100313

Gavva NR, Klionsky L, Qu Y, Shi L, Tamir R, Edenson S, *et al.* (2004). Molecular determinants of vanilloid sensitivity in TRPV1. *Journal of Biological Chemistry* **279**(19)**:** 20283-20295. https://doi.org/10.1074/jbc.M312577200

Gijsen HJM, Berthelot D, Zaja M, Brône B, Geuens I, Mercken M (2010). Analogues of Morphanthridine and the Tear Gas Dibenz[b,f][1,4]oxazepine (CR) as Extremely Potent Activators of the Human Transient Receptor Potential Ankyrin 1 (TRPA1) Channel. *Journal of Medicinal Chemistry* **53**(19)**:** 7011-7020. https://doi.org/10.1021/jm100477n

Gouin O, L'Herondelle K, Buscaglia P, Gall-Ianotto CL, Philippe R, Legoux N, *et al.* (2018). Major role for TRPV1 and InsP3R in PAR2-elicited inflammatory mediator production in differentiated human keratinocytes. *Journal of Investigative Dermatology* **138**(7)**:** 1564-1572. https://doi.org/10.1016/j.jid.2018.01.034

Han Y, Li B, Yin T-T, Xu C, Ombati R, Luo L, *et al.* (2018). Molecular mechanism of the tree shrew's insensitivity to spiciness. *PLoS biology* **16**(7)**:** e2004921-e2004938. https://doi.org/10.1371/journal.pbio.2004921

Harding SD, Sharman JL, Faccenda E, Southan C, Pawson AJ, Ireland S, *et al.* (2018). The IUPHAR/BPS Guide to PHARMACOLOGY in 2018: updates and expansion to encompass the new guide to IMMUNOPHARMACOLOGY. *Nucleic acids research* **46**(D1)**:** D1091-D1106. https://doi.org/10.1093/nar/gkx1121

Ho J-C, Lee C-H (2015). TRP channels in skin: from physiological implications to clinical significances. *Biophysics* **11:** 17-24. https://doi.org/10.2142/biophysics.11.17

Holden C (1989). Cosmetics firms drop Draize test. *Science* **245**(4914)**:** 125-125. https://doi.org/10.1126/science.245.4914.125

Hu H-Z, Xiao R, Wang C, Gao N, Craig C, Jackie W, *et al.* (2006). Potentiation of TRPV3 channel function by unsaturated fatty acids. *Journal of Cellular Physiology* **208**(1)**:** 201-212. https://doi.org/10.1002/jcp.20648

Huang SM, Bisogno T, Trevisani M, Al-Hayani A, Petrocellis LD, Fezza F, *et al.* (2002). An endogenous capsaicin-like substance with high potency at recombinant and native vanilloid VR1 receptors. *Proceedings of the National Academy of Sciences* **99**(12)**:** 8400-8405. https://doi.org/10.1073/pnas.122196999

Iwasaki Y, Morita A, Iwasawa T, Kobata K, Sekiwa Y, Morimitsu Y, *et al.* (2006). A nonpungent component of steamed ginger--[10]-shogaol--increases adrenaline secretion *via* the activation of TRPV1. *Nutritional Neuroscience* **9**(3-4)**:** 169-178. https://doi.org/10.1080/110284150600955164

Julius D (2013). TRP channels and pain. *Annual Review of Cell & Developmental Biology* **29**(1)**:** 355-384. https://doi.org/10.1146/annurev-cellbio-101011-155833

Katzenell S, Cabrera JR, North BJ, Leib DA (2017). Isolation, purification, and culture of primary murine sensory neurons. In. *Innate Antiviral Immunity*, edn, Vol. 1656: Springer. p^pp 229-251.

Kilkenny C, Browne W, Cuthill IC, Emerson M, Altman DG (2010). Animal research: Reporting *in vivo* experiments: The ARRIVE guidelines. *British Journal of Pharmacology* **160**(7)**:** 1577-1579. https://doi.org/10.1111/j.1476-5381.2010.00872.x

Laio A, Gervasio FL (2008). Metadynamics: a method to simulate rare events and reconstruct the free energy in biophysics, chemistry and material science. *Reports on Progress in Physics* **71**(12)**:** 126601-126623. https://doi.org/10.1088/0034-4885/71/12/126601

Lanigan RS, Andersen FA (1999). Final report on the safety assessment of cocamide MEA. *International Journal of Toxicology* **18**(2_suppl)**:** 9-16

Leijon SC, Neves AF, Breza JM, Simon SA, Chaudhari N, Roper SD (2019). Oral thermosensing by murine trigeminal neurons: modulation by capsaicin, menthol and mustard oil. *The Journal of physiology* **597**(7)**:** 2045-2061. https://doi.org/10.1113/JP277385

Liao M, Cao E, Julius D, Cheng Y (2013). Structure of the TRPV1 ion channel determined by electron cryo-microscopy. *Nature* **504**(7478)**:** 107-112. https://doi.org/10.1038/nature12822

Lilley E, Stanford SC, Kendall DE, Alexander SP, Cirino G, Docherty JR, *et al.* (2020). ARRIVE 2.0 and the British Journal of Pharmacology: Updated guidance for 2020: Wiley Online Library.

Lindegren H, Mogren H, El Andaloussi-Lilja J, Lundqvist J, Forsby A (2009). Anionic linear aliphatic surfactants activate TRPV1: A possible endpoint for estimation of detergent induced eye nociception? *Toxicology in Vitro* **23**(8)**:** 1472-1476. https://doi.org/10.1016/j.tiv.2009.06.013

Liu L, Simon S (2003). Modulation of I_A currents by capsaicin in rat trigeminal ganglion neurons. *Journal of neurophysiology* **89**(3)**:** 1387-1401. https://doi.org/10.1152/jn.00210.2002

Müller LJ, Marfurt CF, Kruse F, M.T.Tervo T (2003). Corneal nerves: structure, contents and function.

Experimental Eye Research **76**(5)**:** 521-542. https://doi.org/10.1016/s0014-4835(03)00050-2

McGrath JC, McLachlan EM, Zeller R (2015). Transparency in Research involving Animals: The Basel Declaration and new principles for reporting research in BJP manuscripts. *British journal of pharmacology* **172**(10)**:** 2427-2432. https://doi.org/10.1111/bph.12956

Mertens S, Gilissen L, Goossens A (2016). Allergic contact dermatitis caused by cocamide diethanolamine. *Contact dermatitis* **75**(1)**:** 20-24. https://doi.org/10.1111/cod.12580

Monnot AD, Towle KM, Warshaw EM, Fung ES, Novick RM, Paustenbach DJ*, et al.* (2019). Skin Sensitization Induction Risk Assessment of Common Ingredients in Commercially Available Cleansing Conditioners. *Dermatitis* **30**(2)**:** 116-128. https://doi.org/10.1097/DER.0000000000000445

Nakamura A, Hayakawa T, Kuwahara S, Maeda S, Tanaka K, Seki M*, et al.* (2007). Morphological and immunohistochemical characterization of the trigeminal ganglion neurons innervating the cornea and upper eyelid of the rat. *Journal of Chemical Neuroanatomy* **34**(3)**:** 95-101. https://doi.org/10.1016/j.jchemneu.2007.05.005

Palazzo E, Luongo L, Novellis Vd, Rossi F, Marabese I, Maione S (2012). Transient receptor potential vanilloid type 1 and pain development. *Current Opinion in Pharmacology* **12**(1)**:** 9-17. https://doi.org/10.1016/j.coph.2011.10.022

Shaw DE (2005). A fast, scalable method for the parallel evaluation of distance‐limited pairwise particle interactions. *Journal of computational chemistry* **26**(13)**:** 1318-1328. https://doi.org/10.1002/jcc.20267

Shimizu T, Toriumi H, Sato H, Shibata M, Nagata E, Gotoh K*, et al.* (2007). Distribution and origin of TRPV1 receptor-containing nerve fibers in the dura mater of rat. *Brain Research* **1173**(1)**:** 84-91. https://doi.org/10.1016/j.brainres.2007.07.068

Sipos B, Kojima M, Tiemann K, Klapper W, Kruse ML, Kalthoff H*, et al.* (2005). Lymphatic spread of ductal pancreatic adenocarcinoma is independent of lymphangiogenesis. *Journal of Pathology* **207**(3)**:** 301-312. https://doi.org/10.1002/path.1840

Tarun J, Susan J, Suria J, Susan VJ, Criton S (2014). Evaluation of pH of Bathing Soaps and Shampoos for Skin and Hair Care. *Indian Journal of Dermatology* **59**(5)**:** 442-444. https://doi.org/10.4103/0019-5154.139861

Urban L, Dray A (1993). Actions of capsaicin on mouse dorsal root ganglion cells *in vitro*. *Neuroscience letters* **157**(2)**:** 187-190. https://doi.org/10.1016/0304-3940(93)90733-2

Varga A, Németh J, Szabó Á, McDougall JJ, Zhang C, Elekes K*, et al.* (2005). Effects of the novel TRPV1 receptor antagonist SB366791 *in vitro* and *in vivo* in the rat. *Neuroscience letters* **385**(2)**:** 137-142. https://doi.org/10.1016/j.neulet.2005.05.015

Wang J, Wang Y, Cui W-W, Huang Y, Yang Y, Liu Y*, et al.* (2018). Druggable negative allosteric site of $P2X_3$ receptors. *Proceedings of the National Academy of Sciences* **115**(19)**:** 4939-4944. https://doi.org/10.1073/pnas.1800907115

Wang Y, Li H, Xue C, Chen H, Xue Y, Zhao F*, et al.* (2021). TRPV3 enhances skin keratinocyte proliferation through EGFR-dependent signaling pathways. *Cell Biology and Toxicology* **37**(2)**:** 313-330. https://doi.org/10.1007/s10565-020-09536-2

Wenninger JA, McEwen GN (1997). International cosmetic ingredient dictionary and handbook 7 th Ed. *Cosmetic, Toiletry, and Fragrance Association (CTFA)* **1**(234)

Wu Z, Yang Q, Crook RJ, O'Neil RG, Walters ET (2013). TRPV1 channels make major contributions to behavioral hypersensitivity and spontaneous activity in nociceptors after spinal cord injury. *PAIN*® **154**(10)**:** 2130-2141. https://doi.org/10.1016/j.pain.2013.06.040

Yang F, Xiao X, Wei C, Wei Y, Yu P, Song Z*, et al.* (2015). Structural mechanism underlying capsaicin binding and activation of the TRPV1 ion channel. *Nature Chemical Biology* **11**(7)**:** 518-524.

https://doi.org/10.1038/nchembio.1835

Yang F, Zheng J (2017). Understand spiciness: mechanism of TRPV1 channel activation by capsaicin. *Protein & Cell* **8**(3)**:** 169-177

Yin S, Luo J, Qian A, Du J, Yang Q, Zhou S*, et al.* (2013). Retinoids activate the irritant receptor TRPV1 and produce sensory hypersensitivity. *The Journal of clinical investigation* **123**(9)**:** 3941-3951. https://doi.org/10.1172/JCI66413

Zhao F, Tang Q, Xu J, Wang S, Li S, Zou X*, et al.* (2019). Dehydrocrenatidine Inhibits Voltage-Gated Sodium Channels and Ameliorates Mechanic Allodia in a Rat Model of Neuropathic Pain. *Toxins* **11**(4)**:** 229-243. https://doi.org/10.3390/toxins11040229

Zhou B, Wang Y, Zhang C, Yang G, Zhang F, Yu B*, et al.* (2018). Ribemansides A and B, TRPC6 Inhibitors from *Ribes manshuricum* That Suppress TGF-β1-Induced Fibrogenesis in HK-2 Cells. *Journal of Natural Products* **81**(4)**:** 913-917. https://doi.org/10.1021/acs.jnatprod.7b01037

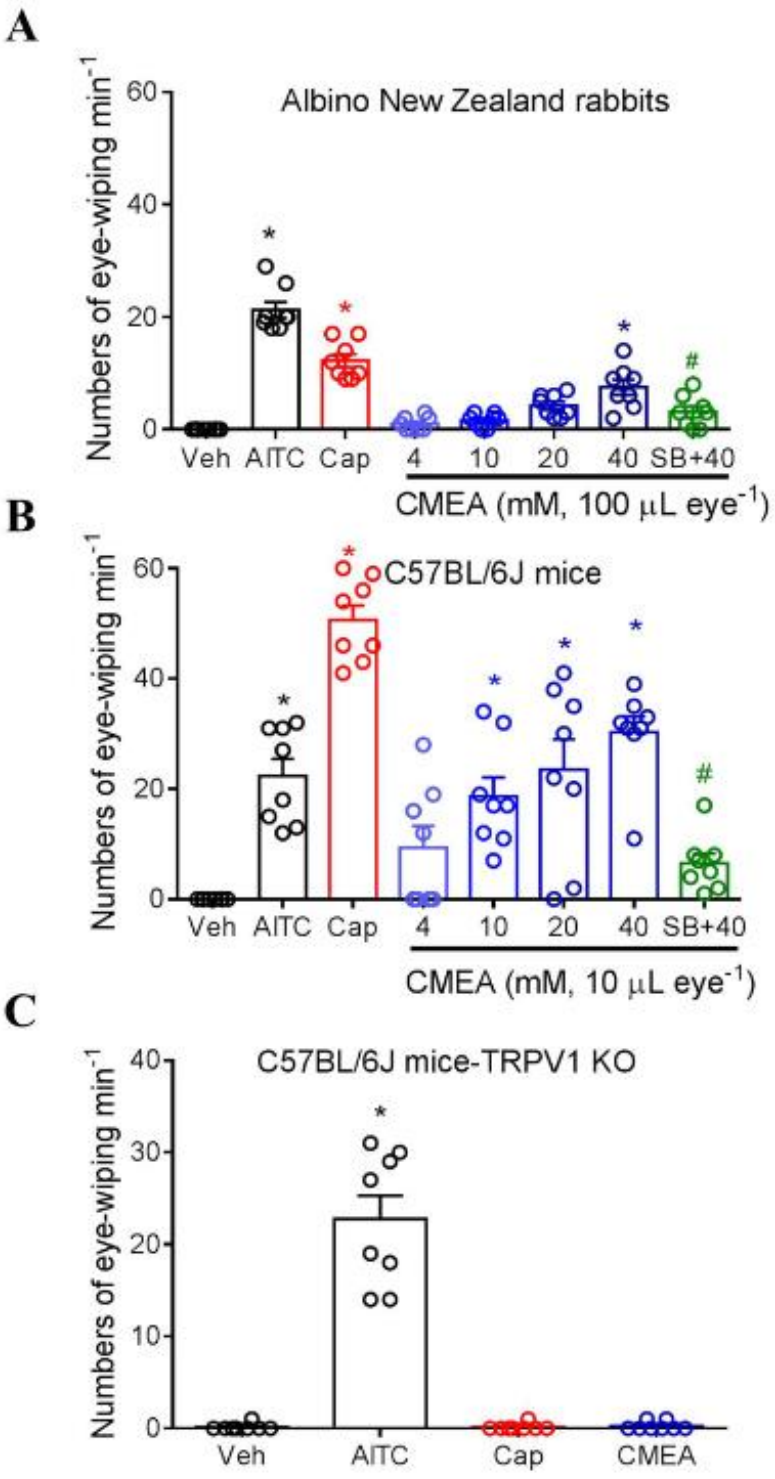

Fig. 1 CMEA produces eye irritation through TRPV1 activation. (**A**) CMEA dose-response (4−40 mM) on the eye-wiping behavior of New Zealand rabbit and response mitigation by TRPV1 inhibitor, SB-366791 (17 mM). The TRPA1 activator, allyl isothiocyanate (AITC, 10 mM) and the TRPV1 agonist, capsaicin (Cap, 1 mM) were used as controls. Each eye received 100 µL of the drug solution.

*, $P < 0.05$, drugs *vs.* Veh (1% DMSO); $^{\#}$, $P < 0.05$, SB-366771+ CMEA (40 mM) *vs.* CMEA (40 mM). (**B**) Mice are more sensitive to CMEA (4−40 mM) in eye-wiping response and largely mitigated by co-instillation of TRPV1 inhibitor, SB-366791 (17 mM), to the eye. *, $P < 0.05$, drugs *vs.* Veh (1% DMSO); $^{\#}$, $P < 0.05$, SB-366791+ CMEA (40 mM) *vs.* CMEA (40 mM). (**C**) TRPV1 knockout (KO) mice are insensitive to CMEA (40 mM) or Cap (1 mM) in the eye-wiping assay, whereas they maintain sensitivity to AITC (10 mM). Each eye receives 10 µL of the drug solution. *, $P < 0.05$, drugs *vs.* Veh (1% DMSO). Data points represent the Mean ± SEM (n = 8 animals).

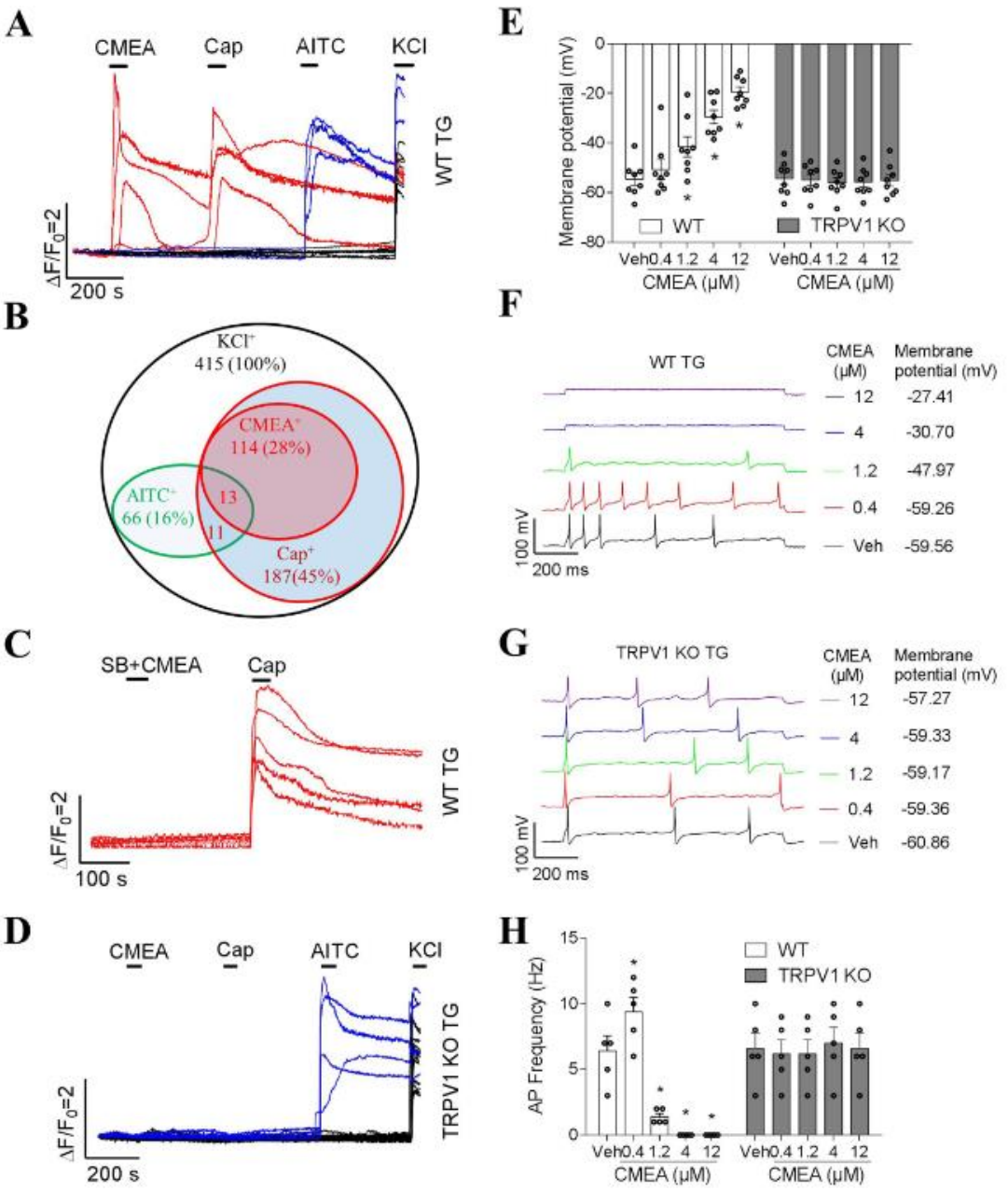

Fig. 2 CMEA stimulates Ca^{2+} influx and affects action potential firing in trigeminal ganglion (TG) neurons through TRPV1 activation. (**A**) Representative traces of CMEA (40 μM), capsaicin (Cap, 1 μM), AITC (100 μM) and KCl (30 mM)-induced Ca^{2+} response in TG neurons. Each trace represents the intracellular Ca^{2+} response of individual neurons as a function of time. Each drug solution was consecutively administrated by bulk perfusion. KCl responsive cells were TG neurons and included in the analysis of drug effects. (**B**) Quantification of Cap, CMEA, allyl isothiocyanate (AITC) responsive neurons from TG neurons isolated from TRPV1 WT mice. (**C**) Representative traces demonstrating SB-366791 (1 μM) suppression of CMEA-induced Ca^{2+} influx in TG neurons. (**D**)

Representative traces of CMEA (40 μM), Cap (1 μM), AITC (100 μM) and KCl (100 mM) affecting Ca^{2+} dynamics in TG neurons acutely isolated from TRPV1 knockout (KO) mice. AITC, but not CMEA or capsaicin, triggered Ca^{2+} influx in TRPV1 KO TG neurons. (**E**) CMEA depolarizes TG neuronal cell membrane potential in isolated from WT but not TRPV1 KO mice. *, $P < 0.05$, CMEA *vs.* Veh (0.1% DMSO) (n = 8 neurons). (**F**) Representative traces showing CMEA mediated alteration in action potential (AP) tonic firing in TG neurons of WT mice. (**G**) Tonic firing of AP in TG neurons isolated from TRPV1 KO mice are unaffected by CMEA. Tonic AP firing are elicited by injection of 100-pA current of 1 s duration. (**H**) Frequency of AP tonic firing in the absence and presence of CMEA in WT and TRPV1 KO TG neurons. CMEA produces a bidirectional response on AP tonic firing in WT TG neurons but does not affect AP firing in TRPV1 KO TG neurons (n = 5 neurons). *, $P < 0.05$, CMEA *vs.* Veh (0.1% DMSO). Data points are the Mean ± SEM.

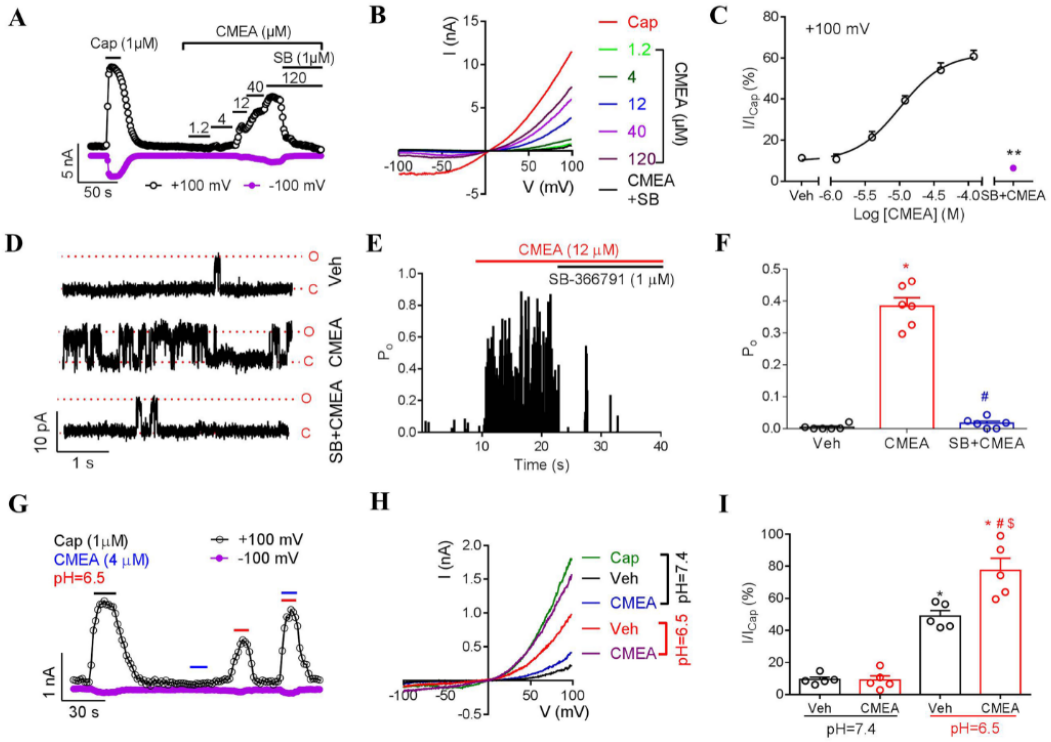

Fig. 3 CMEA directly activates hTRPV1 expressed in HEK-293 cells. (**A**) Representative trace for sequential titration of CMEA-triggered inward (-100 mV) and outward (+100 mV) currents in HEK-293 cells expressing hTRPV1. Capsaicin (Cap, 1 μM) represents the positive control. (**B**) Representative I-V curve illustrating that CMEA activates hTRPV1. (**C**) Concentration-response relationship curve for CMEA activation of hTRPV1 outward current. Currents recorded at +100 mV were normalized to the respective Cap response in each cell. SB-366791 (1 μM) abolished CMEA (120 μM)-induced hTRPV1 currents. *, $P < 0.05$, SB-366791+CMEA *vs.* CMEA, n = 12 cells. (**D**) Representative traces from outside-out recording of TRPV1 single channel gating events recorded at +80 mV in the absence and presence of CMEA (12 μM). (**E**) Quantification of temporal changes in hTRPV1 channel open probability (P_o) after perfusion of the indicated drugs. Data points were binned in 100 ms intervals. (**F**) Quantification of the hTRPV1 channel P_o in the presence of indicated drug treatments. *, $P < 0.05$, CMEA *vs.* Veh (0.1% DMSO); $^{\#}$, $P < 0.05$, SB-366791 + CMEA *vs.* CMEA, n = 6 cells. (**G**) Representative trace for proton (pH = 6.5)-induced inward (-100 mV) and outward (+100 mV) hTRPV1 currents in the absence and presence of CMEA (4 μM). Capsaicin (Cap, 1 μM) was used as positive control. (**H**) Representative I-V curve illustrating that CMEA (4 μM) potentiated proton (pH = 6.5)-induced hTRPV1 currents. (**I**) Quantification of proton-activated TRPV1 currents recorded at +100 mV in the absence and presence of CMEA. Currents were normalized to the respective capsaicin response in each cell. *, $P < 0.05$, pH = 6.5 *vs.* pH = 7.4 (Veh); $^{\#}$, $P < 0.05$, CMEA (pH = 6.5) *vs.* CMEA (pH = 7.4); $^{\$}$, $P < 0.05$, CMEA (pH = 6.5) *vs.* Veh (pH = 6.5), n = 5 cells. Data points represent the Mean ± SEM.

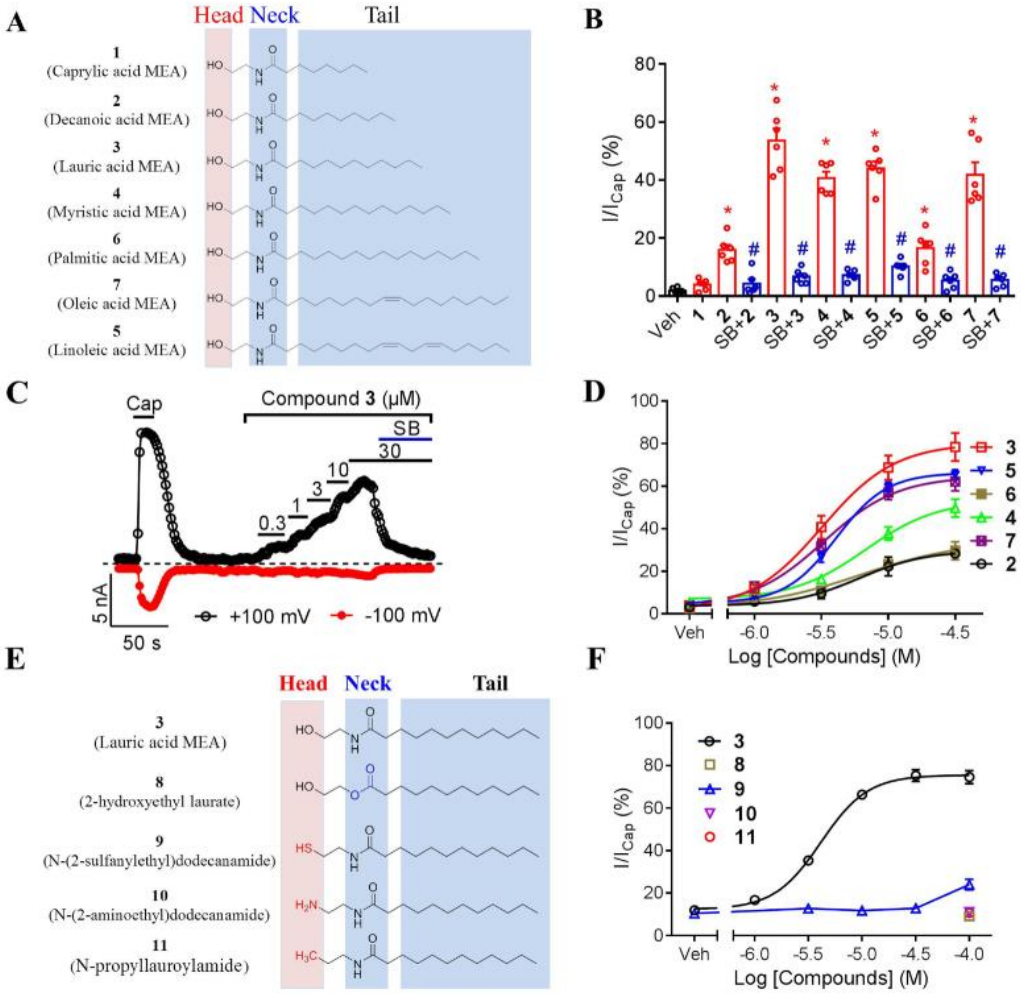

Fig. 4 Structure-activity relationship of compounds 1-11 on hTRPV1 channel activity. (**A**) Structure of compounds **1-7** purified from CMEA. (**B**) Activity of compounds **1-7** (30 μM) on hTRPV1 normalized currents. Compounds **2-7** but not compound **1** elicited hTRPV1 currents in HEK-293 cells, which were suppressed by SB-366791 (1 μM). *, $P < 0.05$, compound *vs.* Vehicle (Veh, 0.1 % DMSO); $^{\#}$, $P < 0.05$, SB-366791 + compound *vs.* compound, n = 6 cells. (**C**) Representative trace hTRPV1 currents before and after sequential elevation of compound **3** at holding potentials of -100 mV (inward current) and +100 mV (outward current) in HEK-293 cells expressing hTRPV1. Capsaicin (Cap, 1 μM) was used as positive control. (**D**) Concentration-response relationship curves of compounds **2-7** activation of hTRPV1. Currents recorded at +100 mV were normalized to the respective Cap response in each cell. n = 10 cells. (**E**) Structures of synthetic analogs of compound **3**, (compounds **8-11**). (**F**) Influence of compounds **8-11** on hTRPV1 activity. All hTRPV1 currents were recorded at +100 mV and normalized to the response to Cap. Compounds **8-11** at concentrations up to 100 μM had no effect on hTRPV1 current. n = 6 cells. Data points represent the Mean ± SEM.

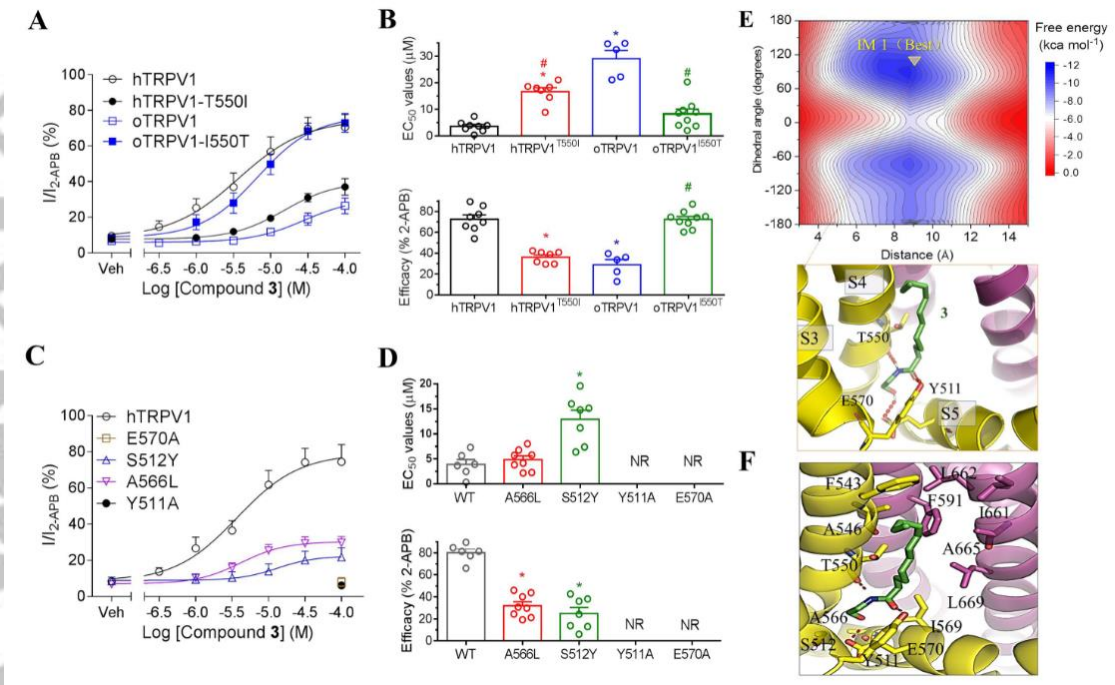

Fig. 5 Molecular model of compound 3 interactions with hTRPV1. (**A**) Relative influences of compound **3** on the activity of hTRPV1, oTRPV1 and mutant channels. Substitution of T550 is critical in defining the differential activity of compound **3** towards hTRPV1 and oTRPV1. (**B**) Potency and efficacy of compound **3** on activation of hTRPV1, oTRPV1 and mutant channels. *, $P < 0.05$, *vs.* hTRPV1; $^{\#}$, $P < 0.05$, *vs.* oTRPV1. (**C**) Influence of compound **3** on hTRPV1 and mutant channels. Currents were normalized to those induced by 3 mM 2-APB in the respective cell. Compound **3** up to 100 μM had no effect on Y511A and E570A mutants. (**D**) Potency and efficacy of compound **3** on activation of hTRPV1 and mutant channels. *, $P < 0.05$, mutants *vs.* WT hTRPV1. NR, no response to compound **3** (100 μM). (**E**) Reconstructed two-dimensional free energy surface (FES, kcal mol^{-1}) based on metadynamics simulations (upper panel) and a close-up view of the optimized compound **3** (green) /rTRPV1 interaction model. The point CV1 indicates the binding mode of compound **3** with the lowest binding free energy. The raw data were obtained by using metadynamics simulations and the free energy surface was generated by Metadynamics Analysis Tool of DESMOND (see methods). Compound **3** is depicted by stick models for emphasis. Red dashed lines indicate hydrogen-bond (H-bond) contacts between the rTRPV1 and compound **3**. (**F**) A close-up view of optimized compound **3**/rTRPV1 interaction mode based on metadynamics simulations. Compound **3** (green) and key residues of TRPV1 are depicted by stick models for emphasis. Red dashed lines indicate hydrogen-bond (H-bond) contacts between the rTRPV1 with compound **3**. The mainchain oxygen atom of T550, rather than the hydroxyl group, made contacts with compound **3**. Data points are the Mean ± SEM (oTRPV1, hTRPV1-E570A, hTRPV1-Y511A groups, n = 5 cells; hTRPV1-S512Y, n = 7 cells; hTRPV1, hTRPV1-T550I, hTRPV1-A566L, n = 8 cells; oTRPV1-I550T group, n = 9 cells). The uneven n number was because of the unsuccessful recordings for some transfected cells.